



Interval multiobjective optimization of structures based on radial basis function, interval analysis, and NSGA-II*

Jin CHENG¹, Gui-fang DUAN^{†‡1}, Zhen-yu LIU², Xiao-gang LI¹, Yi-xiong FENG¹, Xiao-hai CHEN³

(¹State Key Laboratory of Fluid Power Transmission and Control, Zhejiang University, Hangzhou 310027, China)

(²State Key Laboratory of CAD&CG, Zhejiang University, Hangzhou 310058, China)

(³Jingda Machine (Ningbo) Co., Ltd., Ningbo 315033, China)

[†]E-mail: gfduan@zju.edu.cn

Received Sept. 18, 2013; Revision accepted July 22, 2014; Crosschecked Sept. 29, 2014

Abstract: To improve the multiple performance indices of practical engineering structures under uncertainties, an interval constrained multiobjective optimization model was constructed with structural performance indices included in objectives and constraints being functions of the interval uncertain parameters. An algorithm integrating radial basis function (RBF), interval analysis, and non-dominated sorting genetic algorithm (NSGA-II) was put forward to locate the Pareto-optimal solutions to the interval multiobjective optimization model. A series of RBFs were constructed based on the Latin hypercube experimental design (LHED) and finite element analysis (FEA), which were then integrated with interval analysis to compute the interval bounds of the objective and constraint functions under the fluctuation of uncertain parameters. Then the fitness of every individual during the NSGA-II-based optimization could be obtained. The case study on the optimization of the mechanical performance of a press slider with uncertain material properties demonstrated the feasibility and validity of the proposed methodology.

Key words: Interval multiobjective optimization, Uncertainty, Radial basis function (RBF), Interval analysis method, Non-dominated sorting genetic algorithm (NSGA-II)

doi:10.1631/jzus.A1300311

Document code: A

CLC number: TH133.5; TP391

1 Introduction

Although the deterministic structural optimization has been widely studied and applied to some engineering problems, a variety of uncertainties are inherent in the material properties, manufacturing errors, loading conditions, and so on, for the design of

many practical structures, which will result in fluctuations of their mechanical performance. In the worst case, an optimal solution to the deterministic model may become infeasible in engineering practice due to the existence of uncertainties. Hence, it is necessary and important to objectively describe the uncertainties in the modeling of structural optimization problems and develop corresponding uncertain optimization algorithms to obtain solutions applicable in engineering (Ishibuchi and Tanaka, 1990; Schuëller and Jensen, 2008; Guo *et al.*, 2009; Roy *et al.*, 2009; Wang and Huang, 2010; Salehghaffari *et al.*, 2013).

The methods appropriate for modeling the uncertainties in structural optimization include the probabilistic method (Bozkurt Gönen *et al.*, 2012), fuzzy set method (Luo *et al.*, 2006; Cheng *et al.*, 2008), and convex models (Ben-Haim, 1995; Yao *et*

* Corresponding author

[†] Project supported by the National Natural Science Foundation of China (No. 51275459), the Science Fund for Creative Research Groups of National Natural Science Foundation of China (No. 51221004), the National Basic Research Program of China (No. 2011CB706503), the National Science and Technology Major Project of China (No. SK201201A28-01), the Fundamental Research Funds for the Central Universities, and the Innovation Foundation of the State Key Laboratory of Fluid Power Transmission and Control, China

© Zhejiang University and Springer-Verlag Berlin Heidelberg 2014

al., 2011). For the probabilistic method, the uncertain parameters are treated as random variables with their probability distribution functions defined according to the known variation trends of these uncertain parameters (Luo *et al.*, 2011; Tootkaboni *et al.*, 2012). For fuzzy programming, the uncertain parameters are regarded as fuzzy variables, the membership functions of which also need to be known (Liu and Iwamura, 2001). However, it is usually difficult and costly to specify a precise probability distribution or membership function for an uncertain parameter for many practical structures, which greatly restricts the application of these methods in engineering. To overcome the limitations of these methods, convex models, such as ellipsoid (Luo *et al.*, 2009) and interval models (Chen *et al.*, 2012), which only require the bounds of uncertain parameters, have been developed. The interval method has attracted great attention from scholars all over the world, and it has been successfully applied in structural optimization involving uncertain parameters due to the fact that the determination of the lower and upper bounds of a parameter interval is much easier than the determination of a precise probability distribution or membership function (Jiang *et al.*, 2008a; 2008b; 2008c; Wang *et al.*, 2011; Wang and Li, 2012; Li *et al.*, 2013b).

Most of the existing research work on the interval model-based structural optimization aimed at improving only one performance index of a structure, which did not accord with the fact that the practical design of a structure usually needs to improve more than one of its performance indices. Thus, a multi-objective interval optimization model, including multiple performance indices of a structure in the objective and constraint functions, should be established to obtain a structure with good comprehensive performance. For the generality of the interval multiobjective optimization model, the uncertain parameters should be included in both the objective and constraint functions because the performance indices of a structure both in the objectives and constraints may be related with the uncertain parameters. To achieve the objective, an interval multiobjective optimization method for structures was proposed (Li *et al.*, 2013a), which utilized the adaptive Kriging approximations to compute the values of objective and constraint functions. However, the algorithm for solving the interval multiobjective optimization model involves a double-

loop nested optimization procedure, the associated computational cost of which is still prohibitive. The expensive computational cost of the interval optimization algorithm also greatly restricts the application of interval optimization theory and method in the design of practical engineering structures.

To overcome the limitations of the present works, an intuitive idea is to construct approximate models for efficiently computing the structural performance indices of a design scheme and reduce the number of computationally expensive finite element analyses (FEAs) involved in the optimization procedure. Approximate models, such as the back propagation neural network (BPNN) (Cheng *et al.*, 2013), Kriging model (de Oliveira *et al.*, 2013), regression model, and radial basis function (RBF) (Sun *et al.*, 2011; Yilmaz and Kaynar, 2011), which are frequently utilized for the fast estimation of objective and constraint functions in the traditional deterministic optimization, can also be applied to the interval multiobjective optimization of structures. In the presented work, RBF is chosen as a surrogate model of FEA for the computation of objective and constraint functions considering the non-singularity of its coefficient matrix as well as its good fitting precision and computational efficiency (Boyd, 2011). Qasem *et al.* (2012) developed the RBF network based on time variant multiobjective particle swarm optimization for medical disease diagnosis (Qasem and Shamsuddin, 2011a) and proposed several multiobjective hybrid evolutionary algorithms for RBF network design (Qasem and Shamsuddin, 2011b), which demonstrated an appropriate balance between accuracy and simplicity. However, the main concern of the RBF in our work is its fitting precision. The encryption technology of sample points similar to that employed in the outer layer update of Kriging in our previous work (Li *et al.*, 2014) is utilized here to ensure the fitting precision of the RBF. Specifically, the construction of the RBF is an iterative process to achieve a satisfactory fitting precision. The test points for verifying the fitting precision of the current RBF are incorporated into the sample point set for generating the next RBF when the global precision of the current RBF is unsatisfactory, while a small group of sample points within the local region of the maximum error are incorporated into the sample point set when the local precision is unsatisfactory. Furthermore, it has been noted that most uncertainties, such as the fluctuation

of the dimension parameters or material properties of a structure, are usually very small compared with their nominal values in engineering. Hence, the interval analysis method (Qiu and Wang, 2003) is also introduced to calculate the interval bounds of the performance indices in the objective and constraint functions to avoid the nested optimization and further enhance the optimization efficiency since it has been proved to be effective when the uncertainty level of uncertain parameters is small (Jiang *et al.*, 2007b; Wu *et al.*, 2013).

There is no single global solution to a multi-objective problem, and it is often necessary to determine a set of Pareto optimal points. Readers can refer to the reference (Marler and Arora, 2004) for understanding the concept of Pareto optimality. The non-dominated sorting genetic algorithm (NSGA-II) based on the concept of Pareto optimality (Deb, 2001) is utilized for locating the Pareto-optimal solutions to the interval multiobjective optimization model in our work. The fitness value of every individual in the evolution of NSGA is computed by integrating RBF models with the interval analysis method.

In engineering practice, the final design of a structure is chosen from the Pareto-optimal solutions located by numerical algorithms according to the experts' knowledge. The design parameters can be adjusted slightly in consideration of the manufacture and assembly constraints. Thus, it is reasonable to firstly locate the Pareto-optimal solutions to the interval multiobjective optimization model based on approximate models, which provide comprehensive candidate solutions for decision-making. The feasibility and superiority of the final scheme should be further verified by FEA or performance measurement before application in engineering since its parameter values will usually be adjusted on the basis of a chosen Pareto-optimal solution.

2 Multiobjective optimization model of uncertain structures

2.1 Interval multiobjective optimization model of structures

Supposing that all the uncertainties of a structure are described as interval parameters, the general interval multiobjective optimization model can be expressed as

$$\begin{aligned} & \min_{\mathbf{x}} \{f_1(\mathbf{x}, \mathbf{U}), f_2(\mathbf{x}, \mathbf{U}), \dots, f_{N_o}(\mathbf{x}, \mathbf{U})\} \\ & \text{s.t. } g_j(\mathbf{x}, \mathbf{U}) \leq B_j = [b_j^L, b_j^R], \quad j=1, 2, \dots, N_c; \\ & \mathbf{x}_l \leq \mathbf{x} \leq \mathbf{x}_r, \quad \mathbf{x} \in \mathbb{R}^n; \\ & \mathbf{U} = [\mathbf{u}^L, \mathbf{u}^R], \quad U_k = [u_k^L, u_k^R], \quad k=1, 2, \dots, N_u, \end{aligned} \quad (1)$$

where \mathbf{x} is the n -dimensional design vector while \mathbf{x}_l and \mathbf{x}_r are the allowable minimum and maximum vectors of \mathbf{x} , respectively. \mathbf{U} is the N_u -dimensional uncertain vector with all its components U_k being interval numbers. The superscripts "L" and "R" denote the left and right bounds of the interval, respectively. $f_i(\mathbf{x}, \mathbf{U})$ ($i=1, 2, \dots, N_o$) and $g_j(\mathbf{x}, \mathbf{U})$ ($j=1, 2, \dots, N_c$) are the objective and constraint functions, the values of which depend on the design vector \mathbf{x} and the uncertain vector \mathbf{U} , respectively. N_o , N_c , and N_u are the number of objectives, constraints, and uncertain parameters, respectively. B_j is the given interval constant of the j th constraint, which can also be a deterministic value.

2.2 Transformation of interval optimization model into deterministic one

The values of objective and constraint functions in Eq. (1) corresponding to a certain design vector \mathbf{x} are interval numbers since they are functions of the design vector \mathbf{x} and uncertain vector \mathbf{U} . To solve the interval optimization model in Eq. (1), a direct approach is to transform it into a deterministic optimization model so that it can be solved by traditional deterministic optimization algorithms.

2.2.1 Transformation of interval objective functions by interval ranking relation

The interval ranking relation " \prec " proposed by Hu and Wang (2006) has proved to satisfy the basic properties, such as reflexivity, anti-symmetry, and comparability, and it is capable of ranking any two interval numbers, which is defined as follows:

Definition 1 For two interval numbers A and B , there is $A \prec B$ if $m(A) < m(B)$ or $w(A) \geq w(B)$ whenever $m(A) = m(B)$, where $m(A)$ and $m(B)$ are the midpoints of A and B , while $w(A)$ and $w(B)$ are the widths of A and B , respectively. Furthermore, there is $A \prec B$ if $A \prec B$ and $A \neq B$.

According to Definition 1, the midpoints of the intervals determine the order of A and B when $m(A) < m(B)$, while their interval widths determine the order when $m(A) = m(B)$, and the interval with the smaller width is always regarded as the better. As far

as the minimization problem in Eq. (1) is concerned, the minimization of the interval objective functions equals the minimization of both their midpoints and widths. Hence, the objectives in Eq. (1) can be transformed into the following deterministic ones via Hu and Wang (2006)'s interval ranking relation “ \leq ”.

$$\begin{aligned} & \min_{\mathbf{x}} \{f_i^M(\mathbf{x}), f_i^W(\mathbf{x})\}, \\ & f_i^M(\mathbf{x}) = (f_i^L(\mathbf{x}) + f_i^R(\mathbf{x})) / 2, \\ & f_i^W(\mathbf{x}) = (f_i^R(\mathbf{x}) - f_i^L(\mathbf{x})) / 2, \\ & i = 1, 2, \dots, N_o, \end{aligned} \tag{2}$$

where $f_i^M(\mathbf{x})$ and $f_i^W(\mathbf{x})$ are the midpoint and width of the i th interval objective function $f_i(\mathbf{x}, \mathbf{U})$, while $f_i^L(\mathbf{x})$ and $f_i^R(\mathbf{x})$ are its left and right bounds, respectively, the values of which can be obtained by

$$\begin{aligned} f_i^L(\mathbf{x}) &= \min_{U \in I} f_i(\mathbf{x}, U), \\ f_i^R(\mathbf{x}) &= \max_{U \in I} f_i(\mathbf{x}, U), \end{aligned} \tag{3}$$

where $I = \{U | U^L \leq U \leq U^R\}$. As can be seen, the uncertain vector U in the objective functions is eliminated with the introduction of the inlayer optimization processes within the uncertain parameter space.

2.2.2 Transformation of interval constraints by satisfactory degree of interval

The satisfactory degree of an interval (Jiang et al., 2007a) represents the possibility that one interval is smaller than another, which is often utilized for the comparison of various intervals. For intervals A and B , the satisfactory degree $P(A \leq B)$ is a fuzzy definition of the possibility that the interval A is smaller than the interval B , which is computed by

$$\begin{aligned} P(A \leq B) &= \frac{\max\{0, [(A^R - A^L) + (B^R - B^L) - \max(0, A^R - B^L)]\}}{(A^R - A^L) + (B^R - B^L)}. \end{aligned} \tag{4}$$

The constraints are generally made to be satisfied with a certain prescribed confidence level so that the uncertain constraints can be transformed into deterministic ones in probability optimization. Similarly, the interval constraints in Eq. (1) can be trans-

formed into deterministic ones by satisfying them with a certain satisfactory level. Specifically, the uncertain constraints $g_j(\mathbf{x}, \mathbf{U}) \leq B_j$ can be transformed as

$$\begin{aligned} P(G_j \leq B_j) &\geq \lambda_j, \quad j = 1, 2, \dots, N_c, \\ G_j &= [g_j^L(\mathbf{x}), g_j^R(\mathbf{x})], \end{aligned} \tag{5}$$

where G_j is the j th interval constraint at \mathbf{x} resulting from the uncertainties of vector U , $P(G_j \leq B_j)$ is a fuzzy definition of the possibility that the interval G_j is smaller than the interval B_j , and λ_j is a prescribed satisfactory degree level of the j th constraint. $g_j^L(\mathbf{x})$ and $g_j^R(\mathbf{x})$ are the left and right bounds of G_j , respectively, the values of which can be obtained by

$$\begin{aligned} g_j^L(\mathbf{x}) &= \min_{U \in I} g_j(\mathbf{x}, U), \\ g_j^R(\mathbf{x}) &= \max_{U \in I} g_j(\mathbf{x}, U). \end{aligned} \tag{6}$$

As can be seen, the uncertain vector U is eliminated based on Eq. (6) and the transformed constraints in Eq. (5) are deterministic.

2.3 Treatment of multiple objectives and constraints

After the transformation of interval objective and constraint functions into deterministic ones by the interval ranking relation and satisfactory degree of interval, respectively, the multiobjective optimization model of an uncertain structure can be represented as

$$\begin{aligned} & \min_{\mathbf{x}} \{\omega_i (f_i^M(\mathbf{x}) + \alpha_i) / \beta_i + (1 - \omega_i) f_i^W(\mathbf{x}) / \gamma_i\}, \\ & i = 1, 2, \dots, N_o; \\ & \text{s.t. } P(G_j \leq B_j) = P\{[g_j^L(\mathbf{x}), g_j^R(\mathbf{x})] \leq [b_j^L, b_j^R]\} \geq \lambda_j, \\ & j = 1, 2, \dots, N_c, \end{aligned} \tag{7}$$

where $\omega_i \in [0, 1]$ is the weighting factor, different values of which indicate different preferences to the minimization of the midpoints and the width of the objective functions caused by the uncertain parameters. The parameter α_i is introduced to ensure the non-negativity of $f_i^M(\mathbf{x}) + \alpha_i$ while the parameters β_i and γ_i are normalization factors to ensure that the midpoint ($f_i^M(\mathbf{x}) + \alpha_i$) pertains to the same order of magnitude as the width $f_i^W(\mathbf{x})$, the values of which are dependent on

specific optimization problems. Specifically, there is always $\omega_i = \beta_i = 1$ for a deterministic objective function $f_i(\mathbf{x})$ irrelevant to the uncertain parameters since $f_i^W(\mathbf{x}) = 0, f_i(\mathbf{x}) = f_i^M(\mathbf{x})$.

The constrained multiobjective optimization model in Eq. (7) can be further transformed into the following unconstrained optimization model based on the penalty function method:

$$\begin{aligned} \min_{\mathbf{x}} \{ & f_{p_i}(\mathbf{x}) \}, \quad i = 1, 2, \dots, N_o; \\ f_{p_i}(\mathbf{x}) = & \omega_i (f_i^M(\mathbf{x}) + \alpha_i) / \beta_i + (1 - \omega_i) f_i^W(\mathbf{x}) / \gamma \\ & + \psi_j \sum_{j=1}^{N_c} \varphi(P(G_j \leq B_j) - \lambda_j), \quad (8) \\ & j = 1, 2, \dots, N_c, \end{aligned}$$

where $f_{p_i}(\mathbf{x})$ is the penalty function corresponding to the i th objective, ψ_j is the penalty factor of the j th constraint that is often specified as a large value while φ can be represented as

$$\varphi(P(G_j \leq B_j) - \lambda_j) = \{\max[0, -(P(G_j \leq B_j) - \lambda_j)]\}^2. \quad (9)$$

3 Optimization algorithm based on RBF, interval analysis, and NSGA-II

As can be seen from Eqs. (3)–(8), the multi-objective optimization problem of an uncertain structure is finally transformed into a double-level nested optimization problem. The computational cost for the solution of such a nested optimization problem is often extremely expensive since it always requires the computation of a structure’s performance indices involved in the objective and constraint functions for thousands and millions of times. The associated computational costs are usually prohibitive, especially when the structure is represented by a large and detailed finite element model. To overcome this difficulty, RBF is introduced to efficiently compute the structure’s performance indices instead of FEAs. On the other hand, interval analysis is also introduced to eliminate the inlayer optimization for computing the interval bounds of objective and constraint functions caused by the fluctuations of uncertain parameters since it proves to be feasible and valid when all the uncertain parameters considered in the optimization

of a structure are at small uncertainty levels. Finally, a computationally fast NSGA-II is utilized to solve the optimization problem in Eq. (8). Every individual chromosome of the NSGA-II denotes a candidate design vector \mathbf{x} , the fitness value of which can be efficiently obtained based on the RBF models and interval analyses.

3.1 RBF for computing objectives and constraints

3.1.1 Basic idea of the RBF

The basic idea of the RBF is to approximate the response at a point \mathbf{x} for any dimension N_d by the linear superposition of the basic function based on the response values of the sample points $\mathbf{x}_i \in \mathbb{R}^{N_d}$ ($i = 1, 2, \dots, N_s$), where N_s is the number of sample points. Supposing that the N_s sample points with their real response values $f(\mathbf{x}_1), f(\mathbf{x}_2), \dots, f(\mathbf{x}_{N_s})$ are known, the RBF approximation of the following form is employed by

$$\tilde{f}(\mathbf{x}) = \sum_{i=1}^{N_s} \omega_i \phi(\|\mathbf{x} - \mathbf{x}_i\|), \quad \mathbf{x} \in \mathbb{R}^{N_d}, \quad (10)$$

where $\|\cdot\|$ is the Euclidean distance, ω_i is the weight of the i th basic function, and $\phi(\cdot)$ is the Gauss basic function in the expression of

$$\phi(\|\mathbf{x} - \mathbf{x}_i\|) = \exp(-\gamma \|\mathbf{x} - \mathbf{x}_i\|^2), \quad (11)$$

where $\gamma \geq 0$ is a positive constant.

Define matrix

$$\Phi = \begin{bmatrix} \phi(\|\mathbf{x}_1 - \mathbf{x}_1\|) & \cdots & \phi(\|\mathbf{x}_1 - \mathbf{x}_{N_s}\|) \\ \vdots & & \vdots \\ \phi(\|\mathbf{x}_{N_s} - \mathbf{x}_1\|) & \cdots & \phi(\|\mathbf{x}_{N_s} - \mathbf{x}_{N_s}\|) \end{bmatrix}, \quad (12)$$

the RBF that interpolates $((\mathbf{x}_1, f(\mathbf{x}_1)), (\mathbf{x}_2, f(\mathbf{x}_2)), \dots, (\mathbf{x}_{N_s}, f(\mathbf{x}_{N_s})))$ can be obtained by solving

$$\Phi \omega = \mathbf{f}, \quad (13)$$

where $\omega = [\omega_1, \omega_2, \dots, \omega_{N_s}]^T$ and $\mathbf{f} = [f(\mathbf{x}_1), f(\mathbf{x}_2), \dots, f(\mathbf{x}_{N_s})]^T$ are the weighting and real response vectors, respectively. Hence, the weighting vector can be computed by $\omega = \Phi^{-1} \mathbf{f}$ if Φ is a reversible matrix, and

thus the RBF approximate model can be established by Eq. (10).

3.1.2 Encryption technology of sample points

To ensure the precision of the RBFs for computing structural performance indices in objective and constraint functions, the construction of every RBF here is an iterative process based on encryption technology. The multiple correlation coefficient $R^2 =$

$$1 - \frac{\sum_{i=1}^n (y_i - \tilde{y}_i)^2}{\sum_{i=1}^n (y_i - \bar{y})^2}$$

and the relative maximum absolute error $RMAE = \max_{i=1}^n (|y_i - \tilde{y}_i| / STD)$ is utilized to evaluate the global and local precisions of RBF, where $y_i = f(x_i)$ is the performance index of the i th test point obtained by FEA while $\tilde{y}_i = \tilde{f}(x_i)$ is the corresponding value predicted by RBF, \bar{y} and STD are the mean and standard deviation of the test point set, respectively, and n is the number of the points in the test point set. The construction process of an RBF is illustrated in Fig. 1, where $Prec_g$ and $Prec_l$ are desired global and local precisions of RBF while I_{encrypt} is the indicator of encryption. The test points are incorporated into the sample point set when the global precision of the current RBF does not satisfy $R^2 < Prec_g$ while a small group of sample points arranged by the Latin hypercube experimental design (LHED)

within the local region of the biggest RMAE are incorporated into the sample point set when the local precision of the current RBF does not satisfy $RMAE > Prec_l$.

3.2 Interval analysis for determining interval bounds of performance indices

Based on interval mathematics, the interval vector U can be rewritten as

$$U = [u^L, u^R] = u^M + [-1, 1]u^W, \quad (14)$$

where $u^M = (u^L + u^R)/2$ and $u^W = (u^R - u^L)/2$ are the midpoint and width vectors of U , respectively. Hence, the uncertain vector U can be expressed as

$$U = u^M + \delta u, \quad (15)$$

where $\delta u \in [-1, 1]u^W$, $\delta u_k \in [-1, 1]u_k^W$, $k = 1, 2, \dots, N_u$.

Supposing that the uncertainty level of vector U is relatively small, the objective functions in Eq. (1) can be approximated in the uncertain field through the first-order Taylor expansion:

$$f_i(x, U) = f_i(x, u^M + \delta u) \approx f_i(x, u^M) + \sum_{k=1}^{N_u} \frac{\partial f_i(x, u^M)}{\partial u_k} \delta u_k, \quad (16)$$

$i = 1, 2, \dots, N_o.$

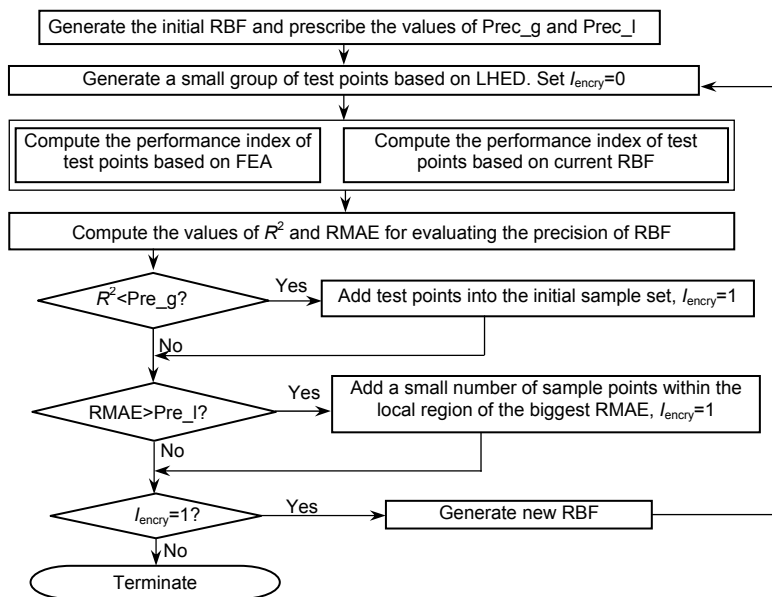


Fig. 1 Flowchart for construction of RBF

Substituting $\delta u_k \in [-1, 1]u_k^W$ into Eq. (16), the interval of the objective function can be obtained through a natural interval extension:

$$F_i(\mathbf{x}, \mathbf{U}) = f_i(\mathbf{x}, \mathbf{u}^M) + \sum_{k=1}^{N_u} \frac{\partial f_i(\mathbf{x}, \mathbf{u}^M)}{\partial u_k} [-1, 1]u_k^W. \quad (17)$$

Thus, the left and right bounds of the i th objective function at the point \mathbf{x} can be obtained by

$$\begin{aligned} f_i^L(\mathbf{x}) &= f_i(\mathbf{x}, \mathbf{u}^M) - \sum_{k=1}^{N_u} \frac{\partial f_i(\mathbf{x}, \mathbf{u}^M)}{\partial u_k} u_k^W, \\ f_i^R(\mathbf{x}) &= f_i(\mathbf{x}, \mathbf{u}^M) + \sum_{k=1}^{N_u} \frac{\partial f_i(\mathbf{x}, \mathbf{u}^M)}{\partial u_k} u_k^W, \quad (18) \\ i &= 1, 2, \dots, N_o. \end{aligned}$$

Similarly, the left and right bounds of the j th constraint function at the point \mathbf{x} can be obtained by

$$\begin{aligned} g_j^L(\mathbf{x}) &= g_j(\mathbf{x}, \mathbf{u}^M) - \sum_{k=1}^{N_u} \frac{\partial g_j(\mathbf{x}, \mathbf{u}^M)}{\partial u_k} u_k^W, \\ g_j^R(\mathbf{x}) &= g_j(\mathbf{x}, \mathbf{u}^M) + \sum_{k=1}^{N_u} \frac{\partial g_j(\mathbf{x}, \mathbf{u}^M)}{\partial u_k} u_k^W, \quad (19) \\ j &= 1, 2, \dots, N_c. \end{aligned}$$

In Eqs. (18) and (19), $f_j(\mathbf{x}, \mathbf{u}^M)$ and $g_j(\mathbf{x}, \mathbf{u}^M)$ can be obtained directly through a single evaluation of the objective and constraint functions at the point $(\mathbf{x}, \mathbf{u}^M)$ while the first derivatives of the objective and constraint functions regarding the uncertain vector can be obtained explicitly based on the RBF models constructed in Section 3.1. As a result, the intervals of the objective and constraint functions at the point \mathbf{x} can be obtained without the time-consuming optimization processes to solve Eqs. (3) and (6) by applying interval analysis, and only a small number of evaluations on the objective and constraint functions are involved.

3.3 NSGA-II for locating Pareto-optimal solutions

The optimization problem of a structure as expressed in Eq. (8) has multiple objectives. There is no single optimal solution but rather a set of compromise solutions named Pareto-optimal to such an optimization problem with multiple conflicting objectives. Among the Pareto-optimal solutions, a solution is

worse with regard to at least another objective if it is better with regard to one objective. Thus, the final scheme of a structure should be determined by designers on the basis of the performance evaluations on various Pareto-optimal solutions. The NSGA-II that integrates a powerful real-coded genetic algorithm (GA) with the concept of Pareto-optimality to produce solutions illustrative of the Pareto-optimal set is proposed to resolve the multiobjective optimization problem in Eq. (8). The algorithm is based on the classification of the individuals in categories according to the concepts of Pareto-optimal set and non-domination. All the non-dominated individuals of a population are assigned rank 1. The remaining individuals are classified again and the non-dominated ones are assigned rank 2. Such a procedure of classification continues until all the individuals of a population are assigned a rank to the effect that individuals with lower ranks are superior to those with higher ranks.

The selection policy employed in NSGA-II is a combination of the rank- and crowding distance-based tournament selection and the recombination-based elite strategy. Supposing that the population size of NSGA-II is Pop, all the individuals are sorted based on non-domination and assigned a crowding distance rank-wise. The basic idea of crowding distance is to compute the Euclidian distance between each individual in the same rank based on their N_o objective values in the N_o -dimensional objective space. The individuals on the boundaries are assigned infinite distances, so that they can be selected all the time. The offspring population generated from the crossover and mutation operations is combined with the current population for the selection operation to generate the next population, so that all the best individuals in previous and current populations can be reserved. Then the $2 \times \text{Pop}$ -sized population is sorted again based on non-domination and only the best Pop individuals are selected. The diversities of individuals are ensured by the crowding distance-based selection in descending order until the population size equals Pop if it exceeds Pop when all the individuals on the same rank are added. The flowchart of the solution procedure of the multiobjective optimization problem in Eq. (8) is illustrated in Fig. 2.

3.4 Description of optimization algorithm

The implementation of the proposed algorithm for solving the multiobjective structural optimization

problem under uncertainties proceeds as follows.

Step 1. Establish the interval multiobjective optimization model of a structure. The requirements for the mechanical properties of the structure are reflected in either objective or constraint functions. The feasible domains of the structural parameters to be optimized and the varying ranges of the uncertainties influencing the mechanical properties of the structure are defined.

Step 2. Perform FEAs to acquire enough sample data, every group of which includes the values of design and interval variables as well as that of objective and constraint functions involved in the optimization model established in Step 1.

Step 3. Develop RBFs for computing the objective and constraint functions by utilizing the sample data acquired in Step 2 as training and test sample points.

Step 4. Construct the approximate deterministic optimization model by integrating interval ranking relation, satisfactory degree of interval, and the RBFs developed in Step 3.

Step 5. Find the Pareto-optimal solutions to the approximate deterministic optimization model by NSGA-II. The RBFs are integrated with interval analysis for efficiently computing the interval bounds of objective and constraint functions. The detailed flowchart of this step is illustrated in Fig. 2.

Step 6. Choose a final parameter scheme of the structure from the Pareto-optimal solutions obtained in Step 5 based on expertise and the requirements or constraints in engineering practice.

4 Application in optimization of a press slider

As the key component of a high speed press, the performance of the slider mechanism, such as stiffness, intensity, and weight, greatly influences the quality of stamping products, the service life of molds, the working performance of the press, and so on. Hence, it is important to optimize the mechanical performance of the slider in the design of a press, the objective of which is to achieve high stiffness and light weight. The material properties of a press slider, such as the elastic modulus and Poisson's ratio, usually fluctuate within some small varying ranges, which will result in the fluctuation of the slider's mechanical performance. Thus, it is an interval multiobjective optimization problem to improve the mechanical performance of a press slider.

This section focuses on the dimension optimization of the slider in a high speed ultra-precision press with double drive and four linkages as illustrated in Fig. 3, the objective of which is to achieve high

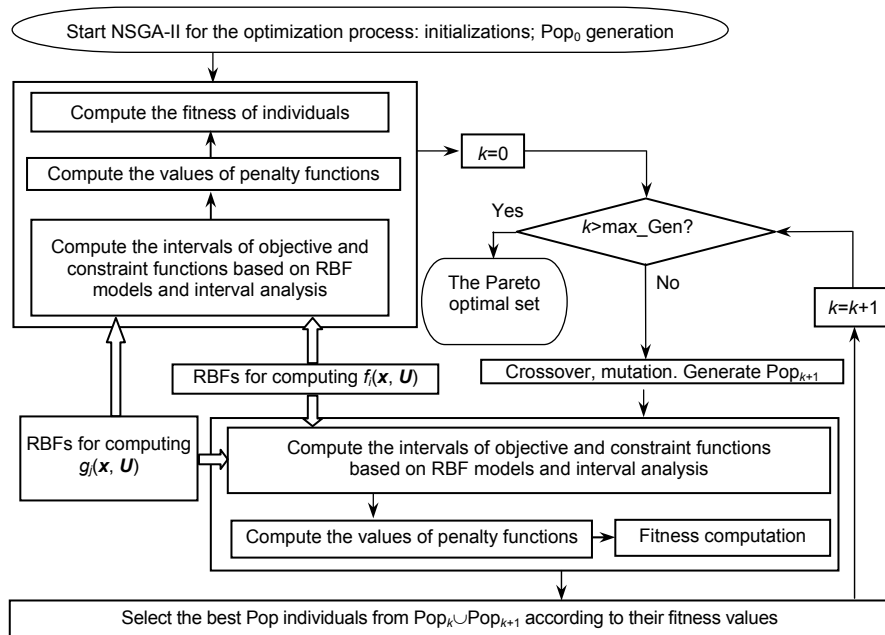


Fig. 2 Flowchart of multiobjective optimization based on RBF, interval analysis, and NSGA-II

stiffness and light weight. The work table of the press is 2700 mm in length and 1000 mm in width. The slider mechanism is composed of a slider, a pin, a linkage, an axle, and a beam, where l and h are the space between two end linkages and the overall height of the slider, respectively. The stiffness of the slider is represented by the linear deflection in the length direction of the slider produced under the stamping force perpendicular to its lower surface, which is denoted as d hereinafter. The measurement of the linear deflection d is illustrated in Fig. 4. Supposing that the deflections at sensors 1, 4, and 7 are measured as δ_1 , δ_4 , and δ_7 , respectively, the linear deflection d is

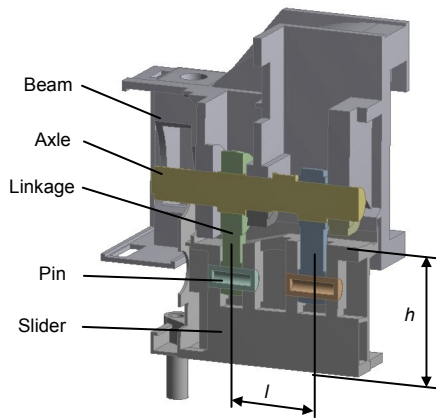


Fig. 3 One fourth solid model of press slider

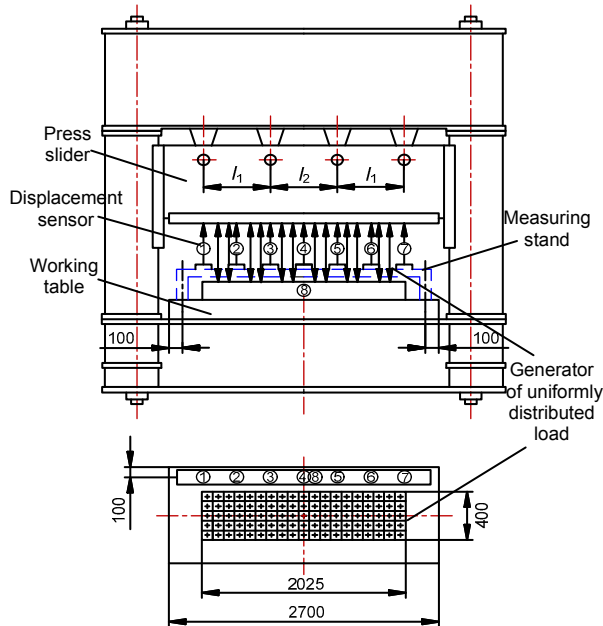


Fig. 4 Diagram for measurement of slider's linear deflection (unit: mm)

computed by $d=[\delta_4-(\delta_1+\delta_7)/2]/(2l_1+l_2)$, and there is $2l_1+l_2=1900$ mm for the press slider investigated here. Note that the linear deflection defined here is a ratio of deflection to length and thus it is dimensionless.

4.1 Construction of interval multiobjective optimization model

As mentioned above, the stiffness of the press slider is described by the linear deflection d . Hence, both objectives of linear deflection and weight should be minimized since the smaller the slider's linear deflection, the larger its stiffness. The maximum stress of the slider should be less than 45 MPa according to expert experience, which is included as a constraint function in the optimization model. The result of sensitivity analysis demonstrates that the dimensions b_1 , b_2 , and b_3 in the cross section (Fig. 5) besides the space l and height h also greatly influence the stiffness and weight of the press slider. Hence, the five dimensions are chosen as design variables, namely, there is $x=(l, h, b_1, b_2, b_3)$. At the same time, the uncertainties of the material properties including the elastic modulus E and Poisson's ratio ν are considered in the optimization of the press slider, namely, $U=(E, \nu)$. The nominal values of E and ν are 1.4×10^5 MPa and 0.25 while their uncertainty level is supposed to be 10% and 8%, respectively. Consequently, the interval multiobjective optimization model of the press slider can be described as

$$\begin{aligned} & \min_x \{d(x, U), w(x)\} \\ & = \min_{l, h, b_1, b_2, b_3} \{d(l, h, b_1, b_2, b_3, E, \nu), w(l, h, b_1, b_2, b_3)\}, \\ & \text{s.t. } \sigma(x, U) = \sigma(l, h, b_1, b_2, b_3, E, \nu) \leq 45 \text{ MPa}, \\ & \quad 500 \text{ mm} \leq l \leq 680 \text{ mm}, \\ & \quad 700 \text{ mm} \leq h \leq 910 \text{ mm}, \\ & \quad 40 \text{ mm} \leq b_1 \leq 120 \text{ mm}, \\ & \quad 20 \text{ mm} \leq b_2 \leq 80 \text{ mm}, \\ & \quad 15 \text{ mm} \leq b_3 \leq 50 \text{ mm}, \\ & \quad E = [1.26 \times 10^5 \text{ MPa}, 1.54 \times 10^5 \text{ MPa}], \\ & \quad \nu = [0.23, 0.27], \end{aligned} \tag{20}$$

where the first objective d indicating the linear deflection and the constraint σ indicating the maximum stress are functions of the design vector x and the uncertain parameter vector U , which fluctuate under the uncertain material properties of elastic modulus E

and Poisson's ratio ν . The second objective w indicating the weight is independent of the uncertain parameter vector U and it is a deterministic objective.

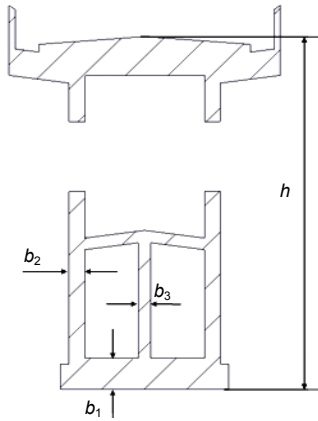


Fig. 5 Cross section of slider

4.2 Optimization procedure

Fig. 6 illustrates the 1/4 FEA model of the press slider that acts as a high fidelity simulation model for computing the slider's mechanical performance. A uniformly distributed load of $B=750$ kN is applied on the lower surface in the 1/4 FEA model of the slider (arrow B) since the whole lower surface of the slider suffers a uniformly distributed load of 3000 kN during the stamping process. The upper beam is connected with four driving oil cylinders and there is a pressure of $A=800$ kN at every connected position (arrow A). The beam is limited at the bottom by the adjusting nuts on the four columns, and thus a fixed support is exerted at its bottom (arrow C). The slider reciprocates up and down during the stamping process, and thus a displacement constraint is exerted at the guiding column, allowing only the vertical movement of the slider (arrow D). Symmetric constraints are applied on two symmetry planes of the 1/4 model (arrows E and F). The mesh model of the 1/4 slider consists of 10685 Solid45 elements and 175976 nodes, the FEA of which is computationally expensive and time-consuming due to the nonlinear contact among different parts.

The global and local precisions $Prec_g$ and $Prec_l$ for terminating the encryption of the sample points are prescribed as 0.95 and 0.05, respectively. The global and local precisions of the final RBF

models for linear deflection, weight, and maximum stress are listed in Table 1, demonstrating that the RBFs are precise enough to be utilized as substitutes for FEA during the interval optimization process of the press slider.

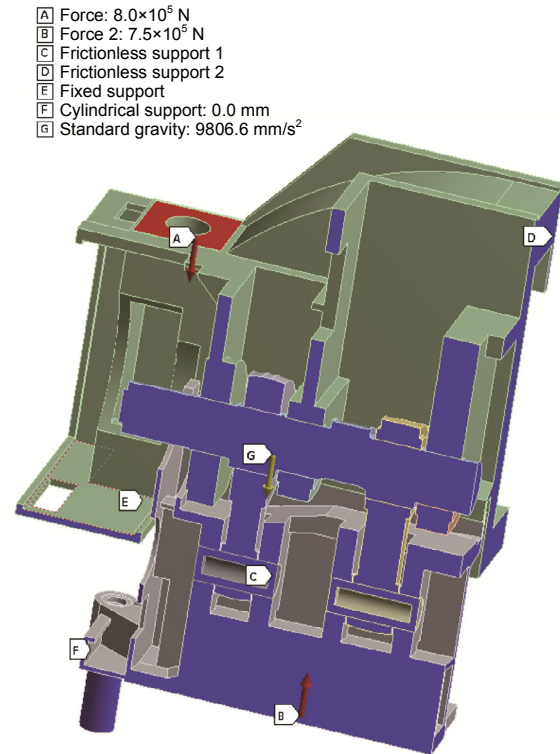


Fig. 6 FEA model of 1/4 press slider: loads and constraints

Table 1 Statistics of RBFs for computing three performance indices of press slider

Statistics	Linear deflection, \tilde{d}	Weight, \tilde{w}	Maximum stress, $\tilde{\sigma}$
R^2	0.9745	0.9628	0.9813
RMAE	0.0489	0.0367	0.0432

Considering that the second objective function $w(x)$ is a deterministic objective, its weighting and normalization factors are set as 1 while its penalty factor is set as 0 to keep its independence from the uncertain parameters. The penalty function of the slider weight is $\tilde{w}_p(x) = \tilde{w}(x)$. Hence, the interval optimization model of the press slider in Eq. (20) can be transformed into the following approximate optimization model based on interval ranking relation and satisfactory degree of interval:

$$\begin{aligned} & \min_x \{ \tilde{d}_p(\mathbf{x}), \tilde{w}(\mathbf{x}) \}, \\ & \tilde{d}_p(\mathbf{x}) = \omega(\tilde{d}^M(\mathbf{x}) + \alpha) / \beta + (1 - \omega)\tilde{d}^W(\mathbf{x}) / \gamma \quad (21) \\ & \quad + \psi \varphi(P((\tilde{\sigma}^L(\mathbf{x}), \tilde{\sigma}^R(\mathbf{x})) \leq 45) - \lambda), \\ & \mathbf{x} = (l, h, b_1, b_2, b_3), \end{aligned}$$

where $\tilde{d}_p(\mathbf{x})$ is the penalty function of the slider's linear deflection d .

Let $\alpha=0, \beta=1.2 \times 10^{-5}, \gamma=1.5 \times 10^{-6}, \omega=0.5, \lambda=1.0$, and $\psi=10000$, the Pareto-optimal solutions to the multiobjective deterministic optimization model in Eq. (21) obtained by NSGA-II is illustrated in Fig. 7, the population, cross and mutation probability, and the maximum generation of the evolution are 100, 0.75, 0.2, and 200, respectively. Point "1" represents the solution that has the lightest weight but the largest linear deflection while Point "2" represents the solution that has the smallest linear deflection but the heaviest weight.

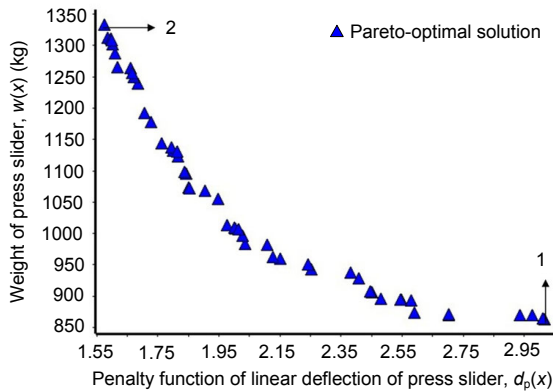


Fig. 7 Pareto-optimal solutions to interval optimization problem of press slider

Table 2 lists 10 Pareto-optimal solutions selected from the Pareto-optimal front in Fig. 7. The 8th solution indicated in boldface is chosen as the final scheme because the manufacturer of the high speed press requires that the linear deflection of the press slider be less than 3.333×10^{-5} and the manufacturing cost should be as low as possible. The final dimensions of the slider are determined as $\mathbf{x}_0=(658, 875, 52, 23, 19)$ to ensure its high stiffness since the results of the sensitivity analysis demonstrated that the smaller spacing l , the bigger height h , and the bigger b_1, b_2 , and b_3 in the cross section will result in the smaller deflection d and thus the larger stiffness of the slider.

The advantage of the interval optimization considering the uncertainties of the material properties over the deterministic one is obvious since the optimal solution obtained by the latter may probably become infeasible in engineering due to the fluctuation of material properties. Specifically, the linear deflection may become larger than 3.333×10^{-5} when the dimensions of the optimal solution to a deterministic optimization model are employed in the production of the press slider.

The computational efficiency of the proposed interval optimization algorithm based on RBF models and interval analysis has been improved exponentially in comparison with the traditional FEA-based nested optimization algorithm. Supposing that the interval optimization model is solved by a traditional double-level nested algorithm based on FEAs, where the outer-layer optimization is implemented by the NSGA-II with the same maximum generation and population size of 200 and 100, respectively, while the inlayer optimization for computing the interval

Table 2 Ten Pareto-optimal solutions to interval optimization problem of press slider

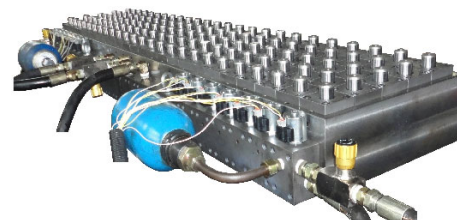
No.	Design vector (l, h, b_1, b_2, b_3)	Weight, w (kg)	Penalty function of deflection, $d_p (\times 10^{-5})$	Interval of deflection, $d (\times 10^{-5})$
1	(652.7, 900.3, 51.7, 71.2, 39.9)	1321.8	1.58	[1.763, 2.213]
2	(648.5, 889.9, 46.1, 67.8, 36.7)	1269.6	1.63	[1.805, 2.273]
3	(648.8, 888.6, 42.7, 61.7, 36.6)	1227.0	1.68	[1.842, 2.328]
4	(615.2, 895.7, 43.1, 52.4, 39.1)	1193.3	1.71	[1.977, 2.449]
5	(645.8, 888.4, 43.4, 42.1, 36.8)	1124.7	1.78	[2.002, 2.504]
6	(653.9, 884.3, 42.6, 33.2, 38.6)	1074.9	1.86	[2.106, 2.630]
7	(615.7, 908.7, 40.6, 25.1, 31.2)	1023.6	1.97	[2.378, 2.902]
8	(658.5, 874.9, 51.3, 22.8, 18.8)	999.17	2.02	[2.419, 2.969]
9	(612.7, 788.7, 41.1, 25.5, 25.2)	946.70	2.24	[2.840, 3.404]
10	(625.3, 757.7, 41.6, 20.2, 16.7)	897.03	2.47	[2.933, 3.599]

bounds of the objective and constraint functions is implemented by GAs with the maximum generation of 200 and the population size of 100. Then a total of 2×10^4 individuals are involved in the outer-layer optimization. As for every individual in the outer-layer optimization, four GA-based optimization procedures are called for computing the interval bounds of the linear deflection d and maximum stress σ , with each procedure involving 2×10^4 individuals. Thus, the traditional nested algorithm based on FEA requires a total of 1.6×10^9 FEAs for solving the interval optimization problem of the press slider in Eq. (20). However, the proposed interval optimization method involves only dozens of FEAs for collecting the sample points during the construction of RBF models. The high efficiency enables the application of the interval optimization method in practical uncertain structures.

4.3 Experimental verification of optimal solution

The experiment was conducted here to measure whether the linear deflection of the slider manufactured according to the scheme obtained by the proposed optimization method meets the requirement of stiffness, specifically, a linear deflection of $d < 3.333 \times 10^{-5}$. To verify the validity of the proposed interval multiobjective optimization approach, an experimental prototype of the high speed press was manufactured with its slider designed according to the optimization result obtained in Section 4.2, namely, $\mathbf{x}_0 = (658, 875, 52, 23, 19)$. The linear deflection of its slider was measured by applying the generator of uniformly distributed load as shown in Fig. 8, which comprised an integrated board of oil cylinders with cartridge valves, a hydraulic station with control valves and accumulators, an electric cabinet with touch screen, several blocks with the same height, and so on. The integrated board in Fig. 8a is 2025 mm in length and 400 mm in width, which comprises 125 oil cylinders uniformly arranged in 5 rows and 25 columns. The centre distance between two adjacent cylinders is 80 mm. For an oil cylinder, the diameters of the piston and its rod are 50 mm and 32 mm, respectively, while the ejection stroke is 20 mm. The 125 cylinders are controlled by 15 groups. The 55 cylinders in the 11 middle columns are controlled by a valve while the 70 cylinders symmetrically arranged in 14 columns at both sides are controlled by 14

valves, namely, every five cylinders in a column are independently controlled by a valve. Therefore, the gradient loading can be realized by an appropriate control of the 15 valves. The nominal working pressure of the hydraulic system is 25 MPa.



(a)



(b)

Fig. 8 Generator of uniformly distributed load: (a) integrated board of oil cylinder; (b) electric cabinet

The arrangement of the uniformly distributed load generator in the press is illustrated in Fig. 4 and Fig. 9. Fig. 4 illustrates that the loading area of the investigated press slider is 2000 mm \times 400 mm, hence, all of the 125 oil cylinders in the integrated board should work simultaneously. When the working pressure of the hydraulic system was set as 12.2 MPa, every oil cylinder could provide a load of 24 kN and the nominal load of 3000 kN uniformly distributed could be applied to the surface of the press slider. As shown in Fig. 4, displacement sensors 1, 3, 5, and 7 were located aligned to the centreline of the four linkages while sensors 2, 4, and 6 were located in the middle of the two neighbouring linkages. All the probes of these displacement sensors are vertically touched the lower surface of the slider (Fig. 9).

Before the start of every experimental run, all the displacement sensors were zeroed. The nominal load of 3000 kN was slowly applied to the lower surface of the press slider in five steps with an increment of 600 kN by adjusting the working pressure of the hydraulic system from 2.44 MPa to 12.2 MPa with an increment of 2.44 MPa at every step. Then the displacements of

all the sensors could be recorded. A total of five experimental runs were conducted. The final displacements of the slider at the seven measuring points were obtained by averaging their corresponding values recorded in five runs, which are listed in Table 3.



Fig. 9 Measurement of prototype's linear deflection

Table 3 Average displacements of five measurement experiments

Average displacement (mm)						
Sensor 1	Sensor 2	Sensor 3	Sensor 4	Sensor 5	Sensor 6	Sensor 7
0.195	0.226	0.243	0.249	0.242	0.224	0.199

As can be seen from Table 3, the average displacements at measuring points 1, 4, and 7 were finally obtained as $\delta_1=0.195$, $\delta_4=0.249$, and $\delta_7=0.199$, respectively. Hence, the linear deflection of the slider was computed as $d=[\delta_4-(\delta_1+\delta_7)/2]/1900=2.737\times 10^{-5}$, which satisfied the requirement of $d<3.333\times 10^{-5}$. It was concluded that the proposed interval multiobjective optimization approach based on RBF models, interval analysis, and NSGA-II can improve the mechanical performance of the press slider and yield an optimal design scheme applicable in engineering practice.

5 Conclusions

To achieve the optimal design of structures with small uncertainties that satisfy the performance requirements in engineering practice, an interval constrained multiobjective optimization model was presented, including interval parameters in both objective and constraint functions, which were transformed into a deterministic unconstrained one based on the interval ranking relation, satisfactory degree of interval,

and penalty function method. A novel algorithm integrating RBF, interval analysis, and NSGA-II was put forward to efficiently solve the multiobjective optimization model. A series of RBF models were constructed for the efficient computation of objective and constraint functions corresponding to given design variables and uncertain parameters while interval analyses were utilized to quickly compute their interval bounds. Then the Pareto-optimal solutions to the multiobjective optimization problem could be finally located by NSGA-II, during the evolution of which the fitness value of every individual was quickly obtained based on RBFs and interval analysis. The advantages of the proposed optimization method over the existing ones were discussed.

The implementation of the proposed methodology was highlighted by the optimization of a press slider's five key dimensions aimed at achieving high stiffness, light weight, and sufficient strength when considering the uncertainty of the elastic modulus and Poisson's ratio. The measurement results on the stiffness of the press slider manufactured according to the chosen Pareto-optimal solution demonstrated the feasibility of the proposed methodology as well as its applicability in engineering practice.

References

- Ben-Haim, Y., 1995. A non-probabilistic measure of reliability of linear systems based on expansion of convex models. *Structural Safety*, **17**(2):91-109. [doi:10.1016/0167-4730(95)00004-N]
- Boyd, J.P., 2011. The near-equivalence of five species of spectrally-accurate radial basis functions (RBFs): asymptotic approximations to the RBF cardinal functions on a uniform, unbounded grid. *Journal of Computational Physics*, **230**(4):1304-1318. [doi:10.1016/j.jcp.2010.10.038]
- Bozkurt Gönen, G., Gönen, M., Gürgen, F., 2012. Probabilistic and discriminative group-wise feature selection methods for credit risk analysis. *Expert Systems with Applications*, **39**(14):11709-11717. [doi:10.1016/j.eswa.2012.04.050]
- Chen, S.M., Yang, M.W., Yang, S.W., et al., 2012. Multicriteria fuzzy decision making based on interval-valued intuitionistic fuzzy sets. *Expert Systems with Applications*, **39**(15):12085-12091. [doi:10.1016/j.eswa.2012.04.021]
- Cheng, J., Feng, Y.X., Tan, J.R., et al., 2008. Optimization of injection mold based on fuzzy moldability evaluation. *Journal of Materials Processing Technology*, **208**(1-3): 222-228. [doi:10.1016/j.jmatprotec.2007.12.114]
- Cheng, J., Liu, Z.Y., Tan, J.R., 2013. Multiobjective optimization of injection molding parameters based on soft

- computing and variable complexity method. *The International Journal of Advanced Manufacturing Technology*, **66**(5-8):907-916. [doi:10.1007/s00170-012-4376-9]
- Deb, K., 2001. Multi-objective Optimization Using Evolutionary Algorithms. John Wiley & Sons, New York, USA.
- de Oliveira, M.A., Possamai, O., Valentina, L.V.O.D., et al., 2013. Modeling the leadership–project performance relation: radial basis function, Gaussian and Kriging methods as alternatives to linear regression. *Expert Systems with Applications*, **40**(1):272-280. [doi:10.1016/j.eswa.2012.07.013]
- Guo, X., Bai, W., Zhang, W.S., et al., 2009. Confidence structural robust design and optimization under stiffness and load uncertainties. *Computer Methods in Applied Mechanics and Engineering*, **198**(41-44):3378-3399. [doi:10.1016/j.cma.2009.06.018]
- Hu, B.Q., Wang, S., 2006. A novel approach in uncertain programming part I: new arithmetic and order relation for interval numbers. *Journal of Industrial and Management Optimization*, **2**(4):351-371. [doi:10.3934/jimo.2006.2.351]
- Ishibuchi, H., Tanaka, H., 1990. Multiobjective programming in optimization of the interval objective function. *European Journal of Operational Research*, **48**(2):219-225. [doi:10.1016/0377-2217(90)90375-L]
- Jiang, C., Han, X., Liu, G.P., 2007a. Optimization of structures with uncertain constraints based on convex model and satisfaction degree of interval. *Computer Methods in Applied Mechanics and Engineering*, **196**(49-52):4791-4800. [doi:10.1016/j.cma.2007.03.024]
- Jiang, C., Han, X., Guan, F.J., et al., 2007b. An uncertain structural optimization method based on nonlinear interval number programming and interval analysis method. *Engineering Structures*, **29**(11):3168-3177. [doi:10.1016/j.engstruct.2007.01.020]
- Jiang, C., Han, X., Liu, G.P., 2008a. A nonlinear interval number programming method for uncertain optimization problems. *European Journal of Operational Research*, **188**(1):1-13. [doi:10.1016/j.ejor.2007.03.031]
- Jiang, C., Han, X., Liu, G.P., 2008b. A sequential nonlinear interval number programming method for uncertain structures. *Computer Methods in Applied Mechanics and Engineering*, **197**(49-50):4250-4265. [doi:10.1016/j.cma.2008.04.027]
- Jiang, C., Han, X., Liu, G.P., 2008c. Uncertain optimization of composite laminated plates using a nonlinear interval number programming method. *Computers and Structures*, **86**(17-18):1696-1703. [doi:10.1016/j.compstruc.2008.02.009]
- Li, F.Y., Luo, Z., Sun, G.Y., et al., 2013a. Interval multi-objective optimisation of structures using adaptive Kriging approximations. *Computers & Structures*, **119**(1):68-84. [doi:10.1016/j.compstruc.2012.12.028]
- Li, F.Y., Luo, Z., Sun, G.Y., et al., 2013b. An uncertain multidisciplinary design optimization method using interval convex models. *Engineering Optimization*, **45**(6):697-718. [doi:10.1080/0305215X.2012.690871]
- Li, X.G., Cheng, J., Liu, Z.Y., et al., 2014. Robust optimization for dynamic characteristics of mechanical structures based on double renewal Kriging model. *Journal of Mechanical Engineering*, **50**(3):165-173. [doi:10.3901/JME.2014.03.165]
- Liu, B.D., Iwamura, K., 2001. Fuzzy programming with fuzzy decisions and fuzzy simulation-based genetic algorithm. *Fuzzy Sets and Systems*, **122**(2):253-262. [doi:10.1016/S0165-0114(00)00035-X]
- Luo, Y.J., Kang, Z., Luo, Z., et al., 2009. Continuum topology optimization with non-probabilistic reliability constraints based on multi-ellipsoid convex model. *Structural and Multidisciplinary Optimization*, **39**(3):297-310. [doi:10.1007/s00158-008-0329-1]
- Luo, Y.J., Li, A., Kang, Z., 2011. Reliability-based design optimization of adhesive bonded steel-concrete composite beams with probabilistic and non-probabilistic uncertainties. *Engineering Structures*, **33**(7):2110-2119. [doi:10.1016/j.engstruct.2011.02.040]
- Luo, Z., Chen, L.P., Yang, J.Z., et al., 2006. Fuzzy tolerance multilevel approach for structural topology optimization. *Computers & Structures*, **84**(3-4):127-140. [doi:10.1016/j.compstruc.2005.10.001]
- Marler, R.T., Arora, J.S., 2004. Survey of multi-objective optimization methods for engineering. *Structural and Multidisciplinary Optimization*, **26**(6):369-395. [doi:10.1007/s00158-003-0368-6]
- Qasem, S.N., Shamsuddin, S.M., 2011a. Radial basis function network based on time variant multi-objective particle swarm optimization for medical diseases diagnosis. *Applied Soft Computing*, **11**(1):1427-1438. [doi:10.1016/j.asoc.2010.04.014]
- Qasem, S.N., Shamsuddin, S.M., 2011b. Memetic elitist Pareto differential evolution algorithm based radial basis function networks for classification problems. *Applied Soft Computing*, **11**(8):5565-5581. [doi:10.1016/j.asoc.2011.05.002]
- Qasem, S.N., Shamsuddin, S.M., Zain, A.M., 2012. Multi-objective hybrid evolutionary algorithms for radial basis function neural network design. *Knowledge-Based Systems*, **27**:475-497. [doi:10.1016/j.knosys.2011.10.001]
- Qiu, Z.P., Wang, X.J., 2003. Comparison of dynamic response of structures with uncertain non-probabilistic interval analysis method and probabilistic approach. *International Journal of Solids and Structures*, **40**(20):5423-5439. [doi:10.1016/S0020-7683(03)00282-8]
- Roy, R., Azene, Y.T., Farrugia, D., et al., 2009. Evolutionary multi-objective design optimisation with real life uncertainty and constraints. *CIRP Annals-Manufacturing Technology*, **58**(1):169-172. [doi:10.1016/j.cirp.2009.03.021]
- Saleghaffari, S., Rais-Rohani, M., Marin, E.B., et al., 2013. Optimization of structures under material parameter uncertainty using evidence theory. *Engineering Optimization*, **45**(9):1027-1041. [doi:10.1080/0305215X.2012.717073]

- Schuëller, G.I., Jensen, H.A., 2008. Computational methods in optimization considering uncertainties—an overview. *Computer Methods in Applied Mechanics and Engineering*, **198**(1):2-13. [doi:10.1016/j.cma.2008.05.004]
- Sun, G.Y., Li, G.Y., Gong, Z.H., et al., 2011. Radial basis functional model for multi-objective sheet metal forming optimization. *Engineering Optimization*, **43**(12):1351-1366. [doi:10.1080/0305215X.2011.557072]
- Tootkaboni, M., Asadpoure, A., Guest, J.K., 2012. Topology optimization of continuum structures under uncertainty—a polynomial chaos approach. *Computer Methods in Applied Mechanics and Engineering*, **201-204**:263-275. [doi:10.1016/j.cma.2011.09.009]
- Wang, Z.J., Li, K.W., 2012. An interval-valued intuitionistic fuzzy multiattribute group decision making framework with incomplete preference over alternatives. *Expert Systems with Applications*, **39**(18):13509-13516. [doi:10.1016/j.eswa.2012.07.007]
- Wang, Z.J., Li, K.W., Xu, J.H., 2011. A mathematical programming approach to multi-attribute decision making with interval-valued intuitionistic fuzzy assessment information. *Expert Systems with Applications*, **38**(10):12462-12469. [doi:10.1016/j.eswa.2011.04.027]
- Wang, Z.L., Huang, H.Z., 2010. A unified framework for integrated optimization under uncertainty. *Journal of Mechanical Design*, **132**(5):051008. [doi:10.1115/1.4001526]
- Wu, J.L., Luo, Z., Zhang, Y.Q., et al., 2013. Interval uncertain method for multibody mechanical systems using Chebyshev inclusion functions. *International Journal for Numerical Methods in Engineering*, **95**(7):608-630. [doi:10.1002/nme.4525]
- Yao, W., Chen, X.Q., Luo, W.C., et al., 2011. Review of uncertainty-based multidisciplinary design optimization methods for aerospace vehicles. *Progress in Aerospace Sciences*, **47**(6):450-479. [doi:10.1016/j.paerosci.2011.05.001]
- Yilmaz, I., Kaynar, O., 2011. Multiple regression, ANN (RBF, MLP) and ANFIS models for prediction of swell potential of clayey soils. *Expert Systems with Applications*, **38**(5):5958-5966. [doi:10.1016/j.eswa.2010.11.027]

中文概要:

本文题目: 基于径向基函数、区间分析和非支配排序遗传算法的结构区间多目标优化

Interval multiobjective optimization of structures based on radial basis function, interval analysis, and NSGA-II

研究目的: 为改善实际工程结构在不确定性条件下的多性能指标, 提供一种高效的区间多目标优化方法。

创新要点: 建立一个目标和约束均为区间不确定性参数函数的区间约束多目标优化模型, 提出并实现基于径向基函数、区间分析和非支配排序遗传算法(NSGA-II)的区间多目标优化算法。

研究方法: 首先, 利用区间序关系将每个区间目标转换为同时优化其中点和半径的确定性双目标, 利用区间可能度法将区间约束转换为确定性约束, 并在此基础上, 利用加权法和罚函数法将每个区间目标的约束优化问题转换为相应的无约束优化问题; 然后, 利用拉丁超立方实验设计和有限元分析构建预测各待优化结构性能指标值的径向基函数; 最后, 将径向基函数、区间分析法与 NSGA-II 相结合, 快速求出转换后确定性无约束多目标优化问题的所有 Pareto 最优解, 并通过考虑材料不确定性的高速压力机滑块机构设计实例验证该方法的有效性。

重要结论: 目标和约束均为不确定性参数函数的区间多目标优化模型能有效反映实际工程中同时改善结构多性能指标的需求。基于径向基函数、区间分析和 NSGA-II 相结合的区间多目标优化算法将传统区间优化模型求解中的嵌套优化过程简化为单层遗传优化过程, 大大提高了求解效率, 并可获得多目标优化问题的所有 Pareto 最优解。

关键词组: 区间多目标优化; 不确定性; 径向基函数; 区间分析法; 非支配排序遗传算法(NSGA-II)